Earth's Future

RESEARCH ARTICLE
10.1029/2020EF001851

Key Points:

- First impact-based forecasting for pluvial foods
- Artificial neural network inundation model significantly cuts calculation time to 0.1% of a physically based model with comparable accuracy
- Forecast with estimates for inundated areas, spreading of contaminants and expected damage could be released 5 min before peak rainfall

Supporting Information:

- Supporting Information S1
- Figure S1
- Figure S2
- Figure S3
- Figure S4
- Figure S5
- Figure S6
- Figure S7
- Figure S8
- Table S1

Correspondence to:
V. Rözer,
v.roezer@lse.ac.uk

Citation:
Rözer, V., Peche, A., Berkhahn, S., Feng, Y., Fuchs, L., Graf, T., et al. (2021). Impact-based forecasting for pluvial floods. *Earth's Future*, *9*, e2020EF001851. https://doi.org/10.1029/2020EF001851

Received 12 OCT 2020
Accepted 4 JAN 2021

Author Contributions:
Conceptualization: V. Rözer
Formal analysis: V. Rözer
Methodology: V. Rözer
Software: V. Rözer
Validation: V. Rözer
Writing – original draft: V. Rözer
Writing – review & editing: V. Rözer

Impact-Based Forecasting for Pluvial Floods

V. Rözer[1,2], A. Peche[3], S. Berkhahn[3], Y. Feng[4], L. Fuchs[5], T. Graf[3], U. Haberlandt[6], H. Kreibich[2], R. Sämann[3], M. Sester[4], B. Shehu[6], J. Wahl[5], and I. Neuweiler[3]

[1]Grantham Research Institute, London School of Economics and Political Science, London, UK, [2]Section Hydrology, Helmholtz Centre Potsdam GFZ German Research Centre for Geosciences, Potsdam, Germany, [3]Institute of Fluid Mechanics and Environmental Physics in Civil Engineering, Leibniz Universität Hannover, Hannover, Germany, [4]Institute of Cartography and Geoinformatics, Leibniz Universität Hannover, Hannover, Germany, [5]Institute for Technical and Scientific Hydrology (itwh) GmbH, Hannover, Germany, [6]Institute of Hydrology and Water Resources Management, Leibniz Universität Hannover, Hannover, Germany

Abstract Pluvial floods in urban areas are caused by local, fast storm events with very high rainfall rates, which lead to inundation of streets and buildings before the storm water reaches a watercourse. An increase in frequency and intensity of heavy rainfall events and an ongoing urbanization may further increase the risk of pluvial flooding in many urban areas. Currently, warnings for pluvial floods are mostly limited to information on rainfall intensities and durations over larger areas, which is often not detailed enough to effectively protect people and goods. We present a proof-of-concept for an impact-based forecasting system for pluvial floods. Using a model chain consisting of a rainfall forecast, an inundation, a contaminant transport and a damage model, we are able to provide predictions for the expected rainfall, the inundated areas, spreading of potential contamination and the expected damage to residential buildings. We use a neural network-based inundation model, which significantly reduces the computation time of the model chain. To demonstrate the feasibility, we perform a hindcast of a recent pluvial flood event in an urban area in Germany. The required spatio-temporal accuracy of rainfall forecasts is still a major challenge, but our results show that reliable impact-based warnings can be forecasts are available up to 5 min before the peak of an extreme rainfall event. Based on our results, we discuss how the outputs of the impact-based forecast could be used to disseminate impact-based early warnings.

Plain Language Summary Pluvial floods are caused by local rain storms with extreme rainfall rates, which leads to immediate flooding of streets and buildings in urban areas. These events are expected to increase in the future due to climate change and growing urban areas. Pluvial floods are directly caused by a rainstorm, which gives citizens and emergency responders usually only a few minutes to act. Existing forecasting systems for pluvial floods are limited to rainfall forecasts that neither provide information about where a flood might occur nor how severe the impacts will be. Here, the main challenge is that current computer models that predict inundation take too long to run to release flood forecasts early enough. We present a new inundation model that can predict inundation for an upcoming flood event in a fraction of the time of existing models. We combine this model with models that predict the spreading of contamination (e.g., from a car accident) and the damage to residential buildings. For a real flood event we can show that this information can be released up to 5 min before the rainfall peak, which gives citizens and emergency responders the opportunities to safe lives and protect important valuables.

1. Introduction

Pluvial, or often referred to as surface water flooding, is directly caused by extreme rainstorms with rainfall rates exceeding the capacity of the urban drainage system. For a long time considered as "nuisance flooding" with little impact, several cities around the globe have been severely impacted by pluvial flooding in recent years. Large-scale pluvial flooding in the Houston area in Texas during hurricane Harvey has led to 68 direct deaths and has caused an estimated damage in the range of USD 90 to 160 billion, making it the second most expensive natural disaster in the history of the United States (Blake & Zelinsky, 2018). Other examples include flooding after a rainstorm in Copenhagen 2011 causing total economic damage of USD 1 billion (DKK 6.2 billion; Wojcik et al., 2013) or a severe rainstorm in Beijing 2012 causing a total economic damage of USD 1.86 billion (CNY 11.6 billion) and 79 fatalities (Wang et al., 2013). But

also smaller, more frequent events such as in Hull in the UK in 2007, where more than 100 mm of rain over a 24 h period caused damage to 8,600 residential buildings and 1,300 businesses (Coulthard & Frostick, 2010) or the pluvial flood in Dortmund, Germany, in July 2008, where local rainfall rates of 200 mm over a time span of 3 h led to a total loss of USD 20 million (EUR 17.2 million; Grünewald et al., 2009), can lead to high cumulative losses over time. With a projected increase in frequency and intensity of heavy rainfall events in many areas around the globe and an ongoing urbanization may further increase the risk of pluvial flooding in the future (Papalexiou & Montanari, 2019; Rosenzweig et al., 2018; Westra et al., 2014).

However, compared to other types of floods, pluvial flooding often occurs at much smaller spatial and temporal scales as they are often caused by convective storms with a high spatial and temporal dynamic. The combination of their small scale and the challenge of accurately predicting pluvial flood events often results in the exclusion of pluvial flood risk from risk management plans and warning systems. However, as pluvial floods often occur in areas that are not obviously prone to flooding and where no flood defenses are in place, timely and detailed warnings can play an important role in protecting people's life and assets (Rözer et al., 2016). For instance, Van Ootegem et al. (2015) found for a pluvial flood event in Belgium that being aware of the risk from pluvial flooding before the water enters a building reduces content damage on average by 90% in the case of basement floods and by 77% in the case of ground floor floods. However, warnings for pluvial floods are challenging, as they require the combination of rainfall forecasts with a high spatial and temporal resolution as well as local information about the urban drainage system, topographic data, land use and soil moisture preconditions. Therefore, warnings for pluvial floods are mostly limited to severe weather warnings containing the expected maximum rainfall intensity on the district level. Only a limited number of more spatially detailed systems (e.g., on the city scale), which also provide information on pluvial flooding itself (i.e., inundation areas), have been implemented in recent years (Henonin et al., 2013; Leitão et al., 2010). The city of Marseilles, France for example created a warning system that links rainfall intensities to locally defined flooding thresholds for floods of different estimated return periods. Warnings are being triggered in case the measured rainfall intensity from radar measurements is above the defined threshold (Deshons & Delrieu, 2002; Parker et al., 2011). In the UK, a new system for extreme rainfall alerts and a surface water flooding forecast was introduced after the pluvial floods in 2007, which is currently further improved (Ochoa-Rodríguez et al., 2018). In addition, several local sensor networks have been developed, which automatically issue a flood warning once a measurement (i.e., observed rainfall intensity, observed water level) exceeds a pre-defined threshold (see Acosta-Coll et al., 2018 for an overview).

While model chains that estimate the current and future pluvial flood risk based on links between rainfall projections and potential impacts such as the expected damage to households or potentially contaminated areas are becoming increasingly available to guide long-term adaptation strategies (Zhou et al., 2012), so far no equivalent short term forecasting systems are available. However, this information can be important for an effective emergency response as it allows to prioritize efforts for an efficient damage reduction and containment given the typically short lead times of pluvial flood events.

In order to use such a model chain in a forecasting system the computational time has to be significantly reduced to provide sufficient lead times that allow for effective short term damage containment and prevention efforts. Here, the high-computational cost and time of two-dimensional (2D) hydro-dynamic models are a key barrier in providing timely inundation predictions. Several methods have been developed to overcome the high-computational costs and time.

For example, Ghimire et al. (2013) suggests cellular-automata models applying generic rules to cells in a regular grid to simulate the spatial-temporal evolution of pluvial flood risk. For a flood early warning system for a harbor in Belgium, Bolle et al. (2018) proposes a simplification of a physically based model. Other approaches include performance improvements of existing 2D physically based models by parallelizing calculations using graphical processing units (GPUs; Judi et al., 2010; Lamb et al., 2009; Neal et al., 2009) and cloud-computing (Morsy et al., 2018). Some studies also try to entirely circumvent the use of inundation models by exploring correlations between radar rainfall data and damage information Spekkers et al. (2013); Grahn and Nyberg (2017). However, up to now the suitability of these models for pluvial flood forecasting systems has not been tested.

In this study, we present a novel impact-based pluvial flood forecasting system using a model chain consisting of a rainfall forecast model, an artificial neural network (ANN) based inundation model, a contaminant transport model and a damage model providing not only predictions of the expected rainfall, but also of the inundated areas, transport of contaminants as well as the expected damage to residential buildings. The data driven ANN model is used to overcome the long computation time of 2D-hydro-dynamic models. To assess the performance of each component of the forecasting system, we first validate the inundation prediction of the ANN model and then analyze the sensitivity of the different outputs of the model chain in regard to the rainfall forecast for a real pluvial flood event. The scope of the study is a proof-of-concept for an impact-based pluvial flood forecasting system including a detailed discussion of the limitations and how the forecasting system can be used as part of a new early warning system for pluvial floods.

The study first introduces the individual model components and then describes how the individual components are linked to an impact based forecasting system. In the case study section, we describe how the forecasting system is set up and validated for an actual pluvial flood event in an urban sub-catchment in the city of Hannover, Germany. In the results section, we present the forecasting skills of the short-time rainfall, inundation and expected damage forecast and how the results compare to available validation data. In the discussion and conclusion, we highlight the challenges and limitations of the described approach and we illustrate how current obstacles can be overcome to provide more meaningful and accurate warnings for pluvial floods including the dissemination of warnings and the possibility for collecting real-time validation data using mobile applications, that are able to safe lives and reduce damage from pluvial flooding.

2. Impact-Based Forecasting System for Pluvial Floods

For the impact-based forecasting system, a short time rainfall forecast model is coupled with a neural-network based urban inundation model, a contaminant transport model and a damage model for residential buildings. In order to reduce the calculation time of the forecasting system, the urban inundation and contaminant transport models use a database of pre-calculated inundation scenarios. This database is set up with simulation results from a hydrodynamic model based on an ensemble of historical and artificial precipitation events and is used for both training of the ANN based urban inundation model and as input for the contaminant transport model.

The outputs of the pluvial flood forecasting system are maps of surface inundation, surface contamination, and damage estimates for residential buildings (which all may be published and continuously updated in a cross-platform mobile application). For the 5 km^2 urban test area used in this study, the runtime of the pluvial flood forecasting system on a desktop PC is less than 5 min, which makes it suitable for a (near-) real-time application. An overview of the complete forecasting system including the potential coupling with a mobile warning system is shown in Figure 1. A more detailed description of all model components is given below.

2.1. Short Time Rainfall Forecast

For the short time rainfall forecast (model component [i] in Figure 1), C-band precipitation radar measurements are corrected, transformed and merged with on the ground measurements from recording stations in real-time to gain the spatial distribution of rainfall intensities of a particular storm (Berndt et al., 2014; Shehu & Haberlandt, 2017). That rainfall intensity information is fed into the forecast model Hyratrac (Krämer et al., 2007) to track the spatio-temporal development of a storm cell. The output of the precipitation forecast model is the location of storm-cells in 5 min intervals giving spatial distributions of rainfall intensities. The model is expected to provide reliable forecasts up to 30 min in advance. In the pluvial flood forecasting system, the rainfall forecast is used as input for the urban inundation and transport models. A detailed description of the precipitation forecast model is given in the Appendix.

2.2. Inundation and Flow Velocity Database

A pre-generated database of flood events (model component [ii] in Figure 1) is used to feed the transport model and to train the ANN inundation model. The database contains an ensemble of historical and

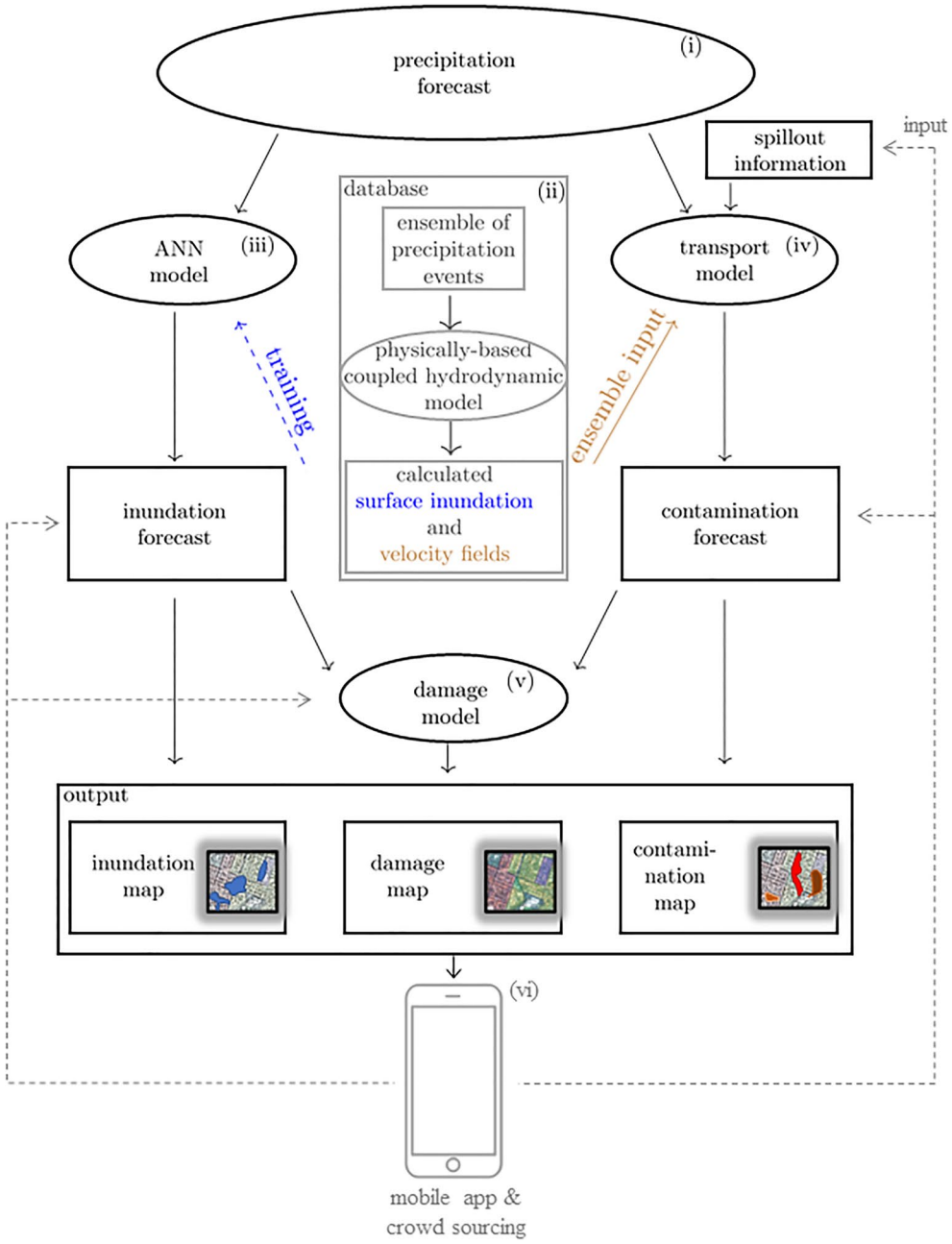

Figure 1. Graphic representation of the impact-based pluvial flood forecasting system.

artificial heavy rainfall events and their corresponding surface inundation and flow velocity fields. The surface inundation and flow velocity fields in the database are modeled, using the heavy rainfall event data as input for a coupled physically based hydrodynamic model representing the urban surface and subsurface flow regimes. It covers a pipe network model for the storm water pipe system that is coupled to a surface flow model. The pipe network model is also coupled to a pipe leakage model to account for storm water pipe leakage. The physically-based hydrodynamic model is validated for a general consistency of the results by comparing the modeled water depths with those of an analytical solution as well against observed flooding for a pluvial flood event that happened on June 22, 2017 in Hannover, Germany (the same event that is used as for the proof of concept study described in this manuscript). For the latter incident reports provided by the local fire brigade are compared to the modeled inundation areas by the physically-based hydrodynamic model. Results of this model such as the spatio-temporal surface inundation as well as the

surface-pipe system-soil-groundwater velocities are stored. A detailed description of the coupled hydrodynamic model and detailed results of the validation exercises are given in the Appendix and are also described in ITWH (2019) and Peche et al. (2019).

2.3. Urban Inundation Model (ANN)

To forecast the spatial distribution of the maximum inundation, an ANN model is used (model component [iii] in Figure 1). ANNs are a machine learning method which uses a structure of edges (synapses) and nodes (neurons) to approximate learned and unknown data and have become a popular approach in recent years to reduce high computation times in flood forecasting (Bermúdez et al., 2018; Chang et al., 2014; Tayfur et al., 2007). The ANN is trained using the ensemble of precipitation events as input and the corresponding modeled spatial distribution of surface inundation information as output from the previously described database. The training of the ANN is done independently from the precipitation forecast. For the inundation forecast the trained ANN predicts the maximum water depth of the surface water inundation for each grid element given the previously described precipitation forecast. The training and prediction capabilities of the ANN model are described in detail in the Appendix and in Berkhahn et al. (2019).

2.4. Transport Model

A transport model (model component [iv] in Figure 1) is used to simulate the spreading of potential surface and subsurface contamination. This information can help to quickly detect areas where contamination of flood water poses a risk to human health and/or leads to an increased risk of severe damage to building structure and contents. The latter has been frequently reported as important damage drivers during flood events (especially in the shape of leaking fuel tanks; Laudan et al., 2017; Thieken et al., 2005). The transport is based on a particle model describing transport of inert contaminants in the pipe system and on the surface. Spreading of contaminant in the subsurface (i.e., soil and groundwater) is not included in the forecast due to the long travel times in this compartment. Input of the transport model are both, information on spills (i.e. location of the contamination source and volume of the contaminants; stemming from for example, crowd sourcing or municipalities), and an ensemble input of velocity fields from the database. The ensemble is chosen using a K-nearest neighbor approach with a metric based on Euclidean distance of precipitation patterns. The transport model generates a superposed ensemble contamination forecast as output in form of maps of the area that has been passed by contaminants. Detailed information about the transport model is given in the Appendix and in Sämann et al. (2019).

2.5. Damage Model

A probabilistic damage model (model component [v] in Figure 1) is used to calculate damages of private households. The model is based on a probabilistic Bayesian zero-inflated beta model (Ospina & Ferrari, 2010) to account for cases, where low water levels and/or damage mitigating measures from household members prevented any monetary damage to the building structure. Input for the damage model are both, a map of maximum water levels of the inundated surface from the ANN inundation model, and a map of the contaminated area generated by the transport model. Additionally the type of building, the number of people living in a household and the household's knowledge about (pluvial) flooding are considered in the model (details about the model inputs for the damage model are described in Section 3.1). The output of the damage model is a map showing the spatial distribution of the estimated damage to residential buildings and the certainty of the estimate in shape of a probabilistic damage distribution. Detailed information about the damage model and its validation is given in the Appendix and in Rözer et al. (2019).

3. Case Study

The complete model chain is applied to hindcast a heavy rainfall event on June 22, 2017 that resulted in widespread pluvial flooding and disruption in the German city of Hannover. Since the developed crowd sourcing model and cross-platform mobile application was not yet operational by the time of the event in Hannover, it could not be included in the proof of concept. The heavy rainfall event was a convective rain

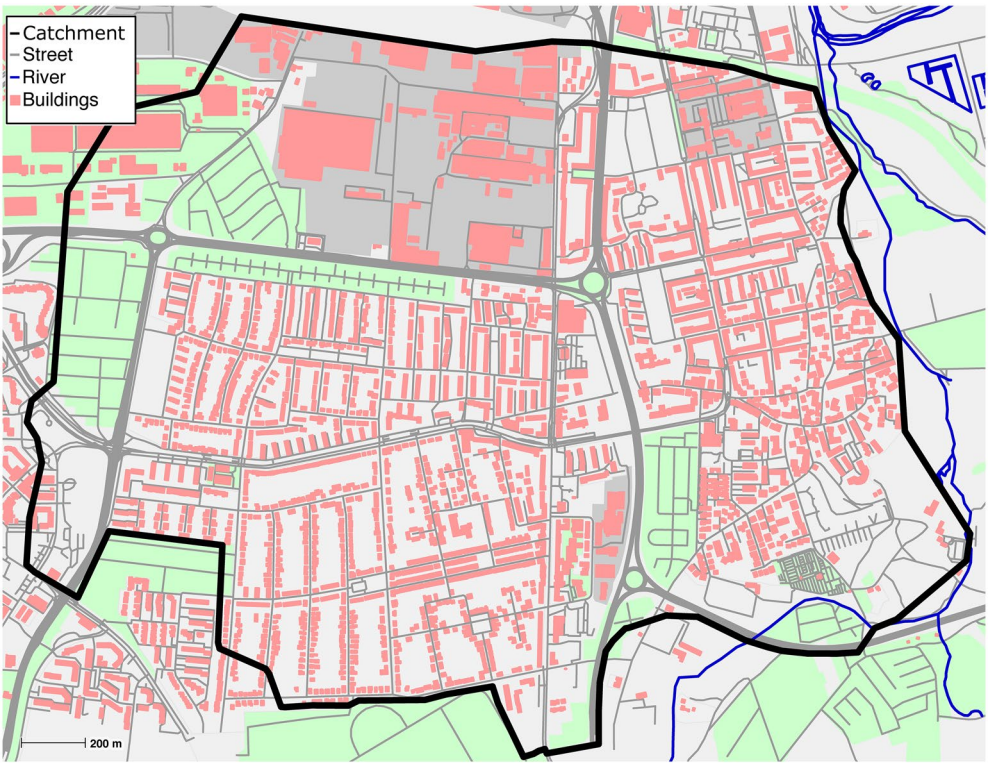

Figure 2. Urban test area in Hannover, Germany.

storm with short and intensive rainfall lasting for 20 min, where most of the rain fell within the first 10 min. The average return period of the event is estimated between 50 and 100 years. The event caused severe disruption of road and rail traffic across Hannover including a black out at the main train station due to flooding of the main power supply. The municipal fire brigade reported over 500 fire runs due to flooded homes.

The following two sections describe how the model chain is set up in the test area in Hannover and how the different outputs of the early warning system are validated for that event.

3.1. Test Area and Model Setup

The test area in Hannover is a 5 km^2 urban subcatchment delineated by two hills at the western boundary and a river at the eastern boundary. The surface slope is relatively flat with an average eastwards slope of 0.6%. Storm water is drained into the river at the eastern boundary by a separate storm water pipe network with a total length of 53 km. The test area has ~10,500 inhabitants with land use dominated by residential housing with small fractions of recreational and industrial use (see Figure 2).

For the simulations with the physically based model that is used to feed the inundation and flow velocity data base, the pipe network in the test area was discretized into 1,200 stormwater pipes. In total, 1,160 manholes and 2,250 street inlets connect the pipe network to the land surface. The land surface was discretized using a total of 1.2 Mio triangle elements with local refinement around street inlets and curb stones. This surface model is based on an elevation model consisting of merged airborne laser scanning data and mobile mapping data with near-street resolution of 0.1–0.5 m (Feng et al., 2018, Appendix). The physically based model was used to simulate in total 529 scenarios based on historical and artificial heavy rainfall events. Regional frequency analysis using 80 rainfall gauges within the radar range of the test area was employed to generate rainfall events with different durations and return periods between 10 and 100 years. Detailed information on how catalog of heavy rainfall events was created can be found in the Appendix. Both the rainfall events and corresponding simulation results are stored in a database and are used to train the ANN

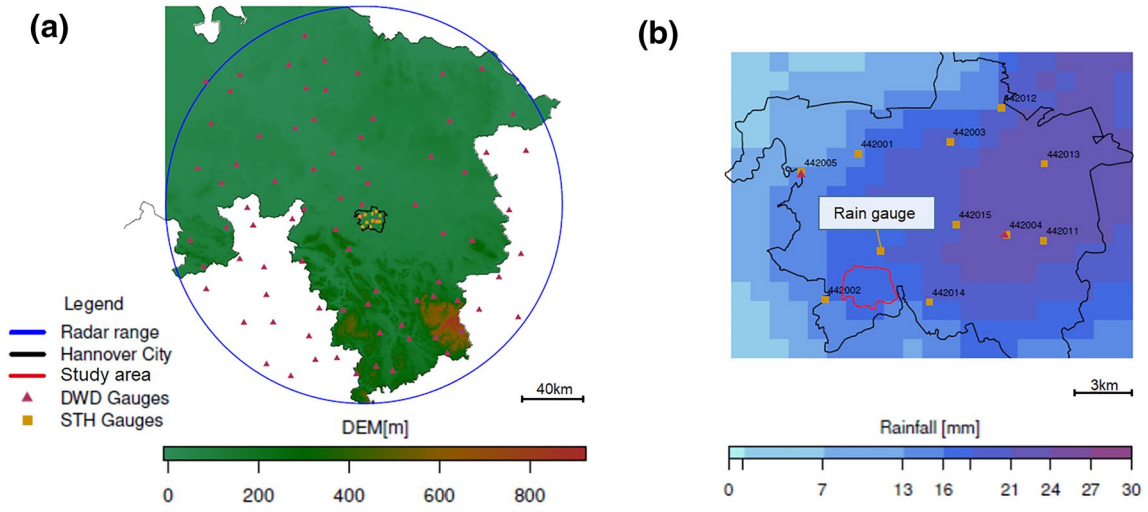

Figure 3. The rainfall data used for the estimation of the rainfall field at 1 km^2 and 5 min resolution and the location of the study area (city of Hannover—black line, test area in Hannover—red line): (a) the overall study area for the forecast model and (b) the close up view of the city of Hannover and the rainfall volume accumulated for 30 min for the convective event on June 22, 2017.

model and provide input for the contaminant transport model. The event on June 22, 2017 used for the hindcast in this study was excluded from the training data set and is therefore not part of the database.

For the precipitation forecast, real-time merging of C-band radar measurements from the station in Hannover Langenhagen and 80 nearby on-the-ground rainfall measurements (radar range and gauge locations are visualized in Figure 3a) are used as input for the storm cell propagation model for the rain forecast.

The forecasted precipitation is used as input for the trained ANN inundation model to predict the water depth on a 5 by 5-m rectangular grid with 103,000 cells. To use the predicted inundation as input for the damage model the maximum water level for each building in the test area is assigned based on the highest water level of all adjoining grid cells.

As no pollution event was reported during the pluvial flood event on June 22 and the mobile application was not yet operational to collect data through VGI, contaminant transport is calculated for a theoretical spill event. The contaminant spreading is calculated based on the forecasted rainfall from the precipitation model. The superposed flow fields are chosen from the database as described in Section 2 and 100.000 contaminant particles are initialized directly before the peak rainfall intensity of the event (18:55 UTC). The injection point at a major street crossing is visualized in Figure 7. This contamination scenario simulates a traffic accident with contaminant spillout (of e.g., oil). The contaminated area is calculated by summing up the area of every grid cell being touched by a contaminant particle.

The damage model is applied using the maximum water level for each residential building from the inundation forecast of the ANN model and information on the expected contamination of each residential building from the contaminant transport model as inputs. A building is considered contaminated, when at least one adjoining grid cell is predicted to be contaminated. The flood duration estimates for each building are empirically derived based on the relationship between the water depth and the flood duration. The average household size in a residential building is estimated based on publicly available census information and the household's knowledge about their flood risk is estimated based on the assumption that all households located within an official flood hazard zone are aware of the risk from flooding. For each affected residential building, first the relative damage (i.e., the percentage of the total value of building structure being destroyed) is calculated and is then multiplied by the estimated total replacement cost of each building to get the absolute damage in EUR. The total replacement cost for each building is calculated by multiplying the estimated living area of each building with the local building price index (BMVI, 2012).

More detailed information on the data that was used to set up the early warning system in the test area in Hannover is provided in the Appendix.

3.2. Validation and Sensitivity Analysis

To test the potential applicability of the presented model chain as part of an impact-based early warning, we assess the accuracy and sensitivity of the provided outputs for the test area in Hannover in two steps. First, we individually test the ability of the ANN to accurately predict the maximum water depth both on the street as well as for each building. For this purpose the maximum water levels are calculated based on rainfall measurements from the nearest gauge (see marked gauge in Figure 3b) and are validated against geo-located photographs from a local newspaper and incident reports provided by the municipal fire brigade for the event on June 22 in Hannover as well as results from the physically based model using the same rainfall measurement as input. This is done to ensure that the inundation predictions both from the data base and provided by the ANN model are reliable enough to be used as input for the subsequent models.

Second, the impact-based forecasting system as a whole is assessed by analyzing the sensitivity of the inundation forecast, contamination forecast and damage estimate given the precipitation forecasts in 5 min time steps (before peak intensity, during peak intensity, after peak intensity) between 18:45 and 19:00 UTC for the event on June 22. The precipitation forecasts for the different time steps are used to first run the ANN inundation model and contaminant transport model and then use the outputs of the two models to run the damage model. The resulting maps (inundation depth for each grid cell, contamination of each grid cell, building structure damage for each residential building) for each forecasting time step are compared to "benchmark" maps that are based on the same model chain but are using the actually measured rainfall from the nearest gauge for each time step instead of the precipitation forecast. In addition, the forecast of the residential building structure damage, as the last output in the model chain, is validated using both long-term average damage information for residential buildings provided by the German Insurers Association (GDV, 2019) and reported damage values to the building structure based on a post event survey of private households in Hannover after the event on June 22. Table 1 gives an overview of the input data and outputs for both the forecast and benchmark model runs. The deviation of the forecasted outputs from the respective benchmarks are used to assess the accuracy and reliability of the early warning system as function of the early warning lead time.

4. Results

According to the validation routine described in the previous section, the results in this section are presented in two parts. In the first part, results from the comparison of the inundation forecast model against photographs and reported damage locations as well as against model results from the physically based model are presented. In the second part, all components of the model chain are evaluated by comparing their sensitivity to the accuracy of the rainfall forecast for different forecasting lead times.

4.1. ANN Inundation Model

The ANN model predictions of the maximum water levels for the June 22, 2017 event (based on data from the closest rain gauge, shown in Figure 3) as well as the location of reported incidents and press photographs are given in Figure 4. The location of reported incidents generally align well with the inundation prediction. Both locations where damage incidents were reported lie within an area with relatively large maximum water levels (0.1–0.6 m). The water levels shown on press photographs from that event also agree qualitatively well with predicted maximum water levels from the ANN model: The photographs indicated in yellow show water levels in the range of a dozen cm (scooter tire-high, ankle-high) which agrees with the prediction of the maximum water levels on the photos which are in the range of 0.1–0.3 m. Photographs indicated in green show smaller water levels (shoe sole-high, inundated/wetted streets, splash from tram). For this location, the ANN predicted water levels are in the range of 0.02–0.3 m. The photographs indicated in purple show a roundabout with a wetted street (water levels are estimated to be in the few cm-range), which again agrees well with the predicted maximum water levels of 0.02–0.1 m for this location. However, since there is no information available at what time the photographs have been taken, this comparison rather provides a qualitative indication of the accuracy of the ANN inundation prediction than a full quantitative validation. Locations that show very high water levels (>1 m) are sinks in the elevation model representing house entrances and parking spaces below street level (see photographs indicated in gray in Figure 4).

Table 1
Overview of Model Components, Their Inputs for the Forecast and Benchmark Models as Well as the Outputs and Computation Time

Model component	Output	Forecast	Benchmark	Comp. Time forecast [mm:ss] [a]	Comp. Time benchmark [mm:ss] [a]
Rainfall forecast	Cumulative rainfall volume [mm]	C-Band Radar merged with 80 gauge stations within a 128 km radius	Closest rain gauge (<1 km away)	00:40	–
Inundation model	Maximum water depth [m]	ANN model using rainfall forecast	Physically based model using benchmark rainfall	00:20	260:00
Contaminant transport model	Contaminated area [ha]	Ensemble of pre-calculated flow fields selected based on forecast rainfall input	Flow field calculated with physically based model with benchmark rainfall	03:30	00:39
Damage model	Damage to building structure [EUR] (residential)	Maximum water depth from ANN model Contaminated area forecast Additional data on: building location and type, average household size, flood zones	Maximum water depth from ANN model with benchmark rainfall Contaminated area from benchmark contaminant transport model Additional data on: building location and type, average household size, flood zones	00:28	00:17
Total	–	–	–	04:58	260:56

Abbreviation: ANN, artificial neural network.
[a]on a standard desktop PC.

For further evaluation of the inundation forecast model (ANN), predicted maximum water levels at each building are compared with the maximum water levels at each building calculated with the physically based model. This is done to assess the quality of the predicted information that is passed on to the damage model. Results are given in Figure 5. Both results represent the June 22, 2017 event. Maximum water levels are compared for 2,186 buildings in the test area. The results of the inundation forecast and physically-based model deviate in 82% by less than ± 0.06 m and in 67% by less than ± 0.04 m. Figure 5a shows the spatial distribution of the deviations for all buildings in the test area. While no spatial clustering of strong over- or underestimations of the maximum water depth is visible, the distribution of deviations show a general trend of the inundation prediction model to overestimate maximum water levels compared to the physically based model (Figure 5b). This trend also reflects on the maximum overestimation, which is five times larger (0.55 m) than the maximum underestimation of −0.11 m. In a flood prediction model, such a trend toward an overestimation of maximum water levels is not necessarily problematic because non/underprediction of a flood event might otherwise lead to under-preparedness of local emergency responders and the general public.

4.2. Forecast Results

The results of all components of the forecast model chain for the pluvial flood event on June 22, 2017 are given in Figure 6. For the rainfall forecast, the merged radar data agree well with the rainfall records from the rainfall gauge, however there is a 10% bias in regard to the total event volume (Figure 6a). This small deviation is acceptable as the gauge and radar measurements differ both on the spatial scale and the way precipitation is measured. While the peak intensity has been captured well by the radar forecast, the volume after the peak is clearly underestimated. The results of the forecast at 18:45 UTC (5 min before the peak) and 18:50 UTC (at the first peak), show that the first peak is well captured. However, the total rainfall volume is underestimated by almost 50% (Figure 6a). Similarly, the resulting deviation from measured rainfall compared to forecasts at 18:55 UTC (at the second peak) and 19:00 UTC (after the peak) is relatively large. However, the real-time integration of gauge measurements from previous time steps successfully reduced the underestimation to 40% and 15% respectively. Even though the cumulative rainfall volume is clearly underestimated, the correlation of the forecast is well above the threshold for predictability (0.37) (see Figure 4

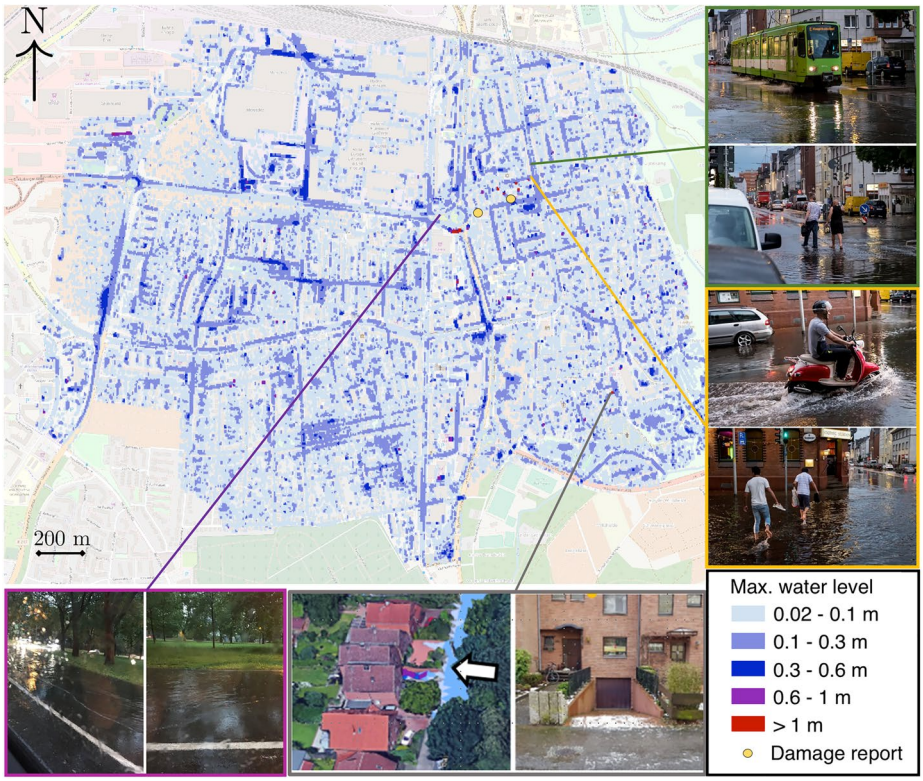

Figure 4. Results of the ANN-predicted maximum water levels (based on data from rain gauge measurements) compared with press photographs (source: http://www.haz.de/Hannover/Fotostrecken-Hannover/So-haben-HAZ-Leser-das-Unwetter-erlebt#n24090935-p58HAZ, access date: 04.04.2018). The photos show four different locations of local flooding. The different locations are framed in different colors (Yellow: estimated flood depth ~10–15 cm; Green: estimated flood depth <5 cm; Purple: estimated flood depth <5 cm; Gray: estimated flood depth >1 m. Yellow dots indicate the location of two incident reports from the municipal fire brigade confirming water has entered a building at these locations. ANN, artificial neural network.

in the Appendix). Forecasted inundation in the shape of the mean surface water level is given in Figure 6b. Clearly, results correlate with results from the rain forecast. For later time steps the inundation forecast captures the inundation well compared to measured rainfall inputs, while earlier forecast times lead to an underestimation of the inundation.

The results of the contaminant transport model, measured as the contaminated area are shown in Figure 6c and Figure 7. At peak rainfall (18:55 UTC), the forecast model considerably overestimates the contaminated area by 9 ha compared to the contaminated area of 2.76 ha of the result using rainfall measurements from the nearest rain gauge (see Figure 3b). There is a 97.7% spatial overlap between the forecasted area and the benchmark result. Five minutes after the rainfall peak (19:00 UTC), results still show a high overestimation of the contaminated area (10.1 ha) and again a high spatial overlap (98.26%) between forecast and benchmark maps.

The spatially aggregated results of the damage model mostly follow those of the inundation forecast with a gradual increase of the average damage per building with decreasing lead times. Compared to mean damage estimates using the inundation input from measured rainfall information (EUR 4604 for radar and EUR 4662 for gauge), the mean damage per building is slightly overestimated for later time steps (EUR 4677 at 19:00 UTC) (Figure 6d). This is caused both by higher mean water levels and the higher number of exposed buildings as well as some of the buildings being modeled as contaminated. Overall, the estimates of the average building estimates show to be relatively robust to the deviations in the predicted mean water level with differences in the mean building damage of only EUR 123 and EUR 65 between the earliest forecast (18:45 UTC) and the gauge and radar benchmarks respectively. Same is true for 90% predictive intervals where both upper and lower bounds vary by less than EUR 100. For the damage prediction of individual

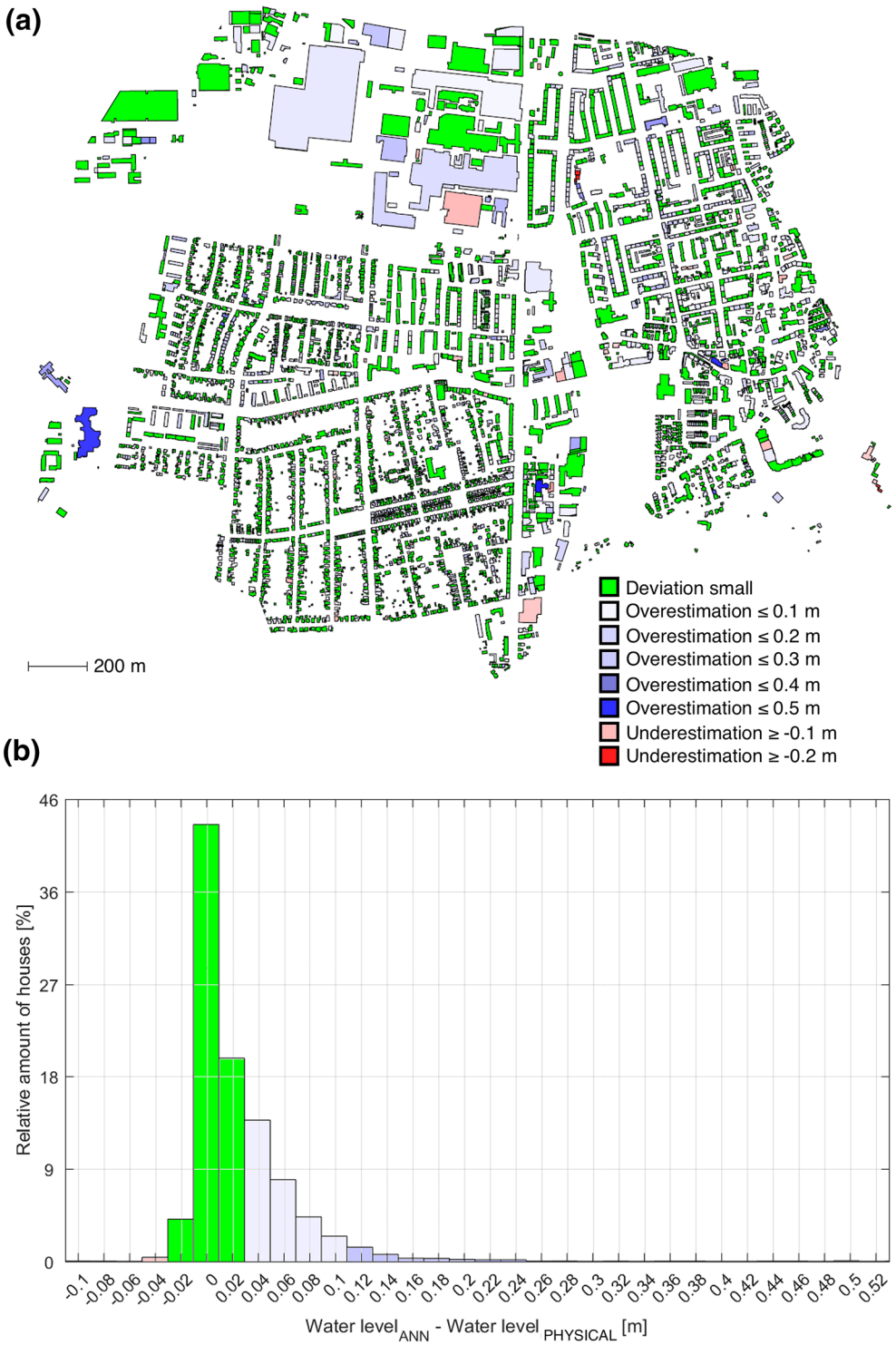

Figure 5. Spatial distribution (a) and histogram (b) of deviation of maximum water levels directly at the houses between ANN and the results from the physically based model (PHYSICAL). ANN, artificial neural network.

residential buildings, no strong spatial deviations between the different forecasting time steps are visible (Figures 7a–7c). Similarly, no bias toward a strong over- or under-prediction of individual building damage is visible although earlier forecasting steps tend to slightly underestimate damage to residential buildings (Figure 7d). Apart from the relative accuracy of the damage estimates based on different inundation inputs,

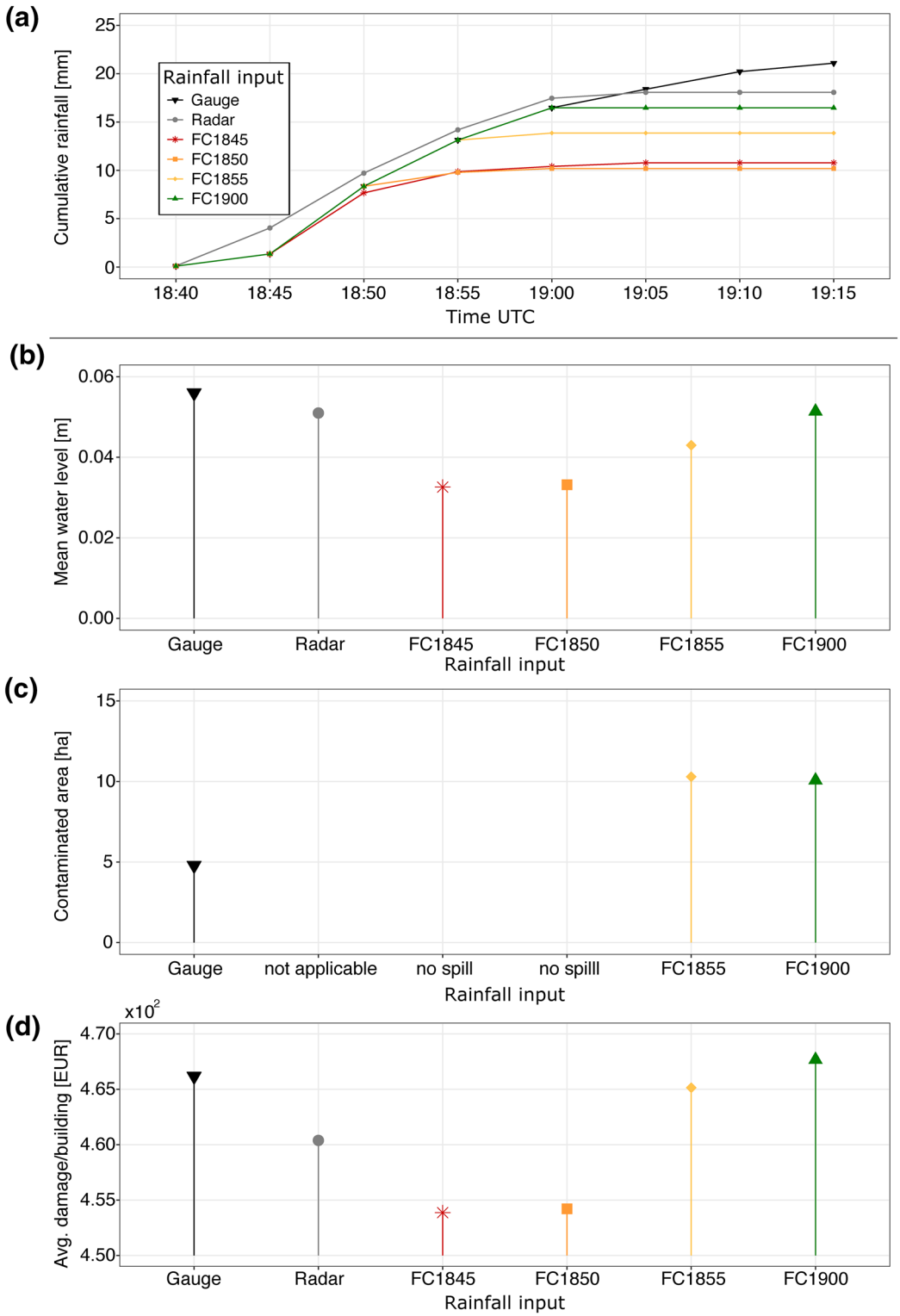

Figure 6. (a) Cumulative rainfall for the June 22, 2017 event from measurements (Gauge and Radar) and four different rain forecast times (FC). FC refers to the time (UTC) a rainfall forecast was modeled based on the observed rainfall information that was available at that point in time; e.g. FC1855 uses rainfall observations from 18:40 to 18:55 UTC to predict cumulative rainfall from 18:55 UTC onwards. (b) Results of the inundation model is based on measured (Gauge, Radar) and forecasted rain events (FC1845 - FC1855). The plot shows the mean of the predicted maximum water level across all inundated cells in the test area. (c) The contaminated area is based on measurements from the closest rain gauge as well as on forecasts (FC1855 and FC1900). (d) Results of the damage model based on measured and forecasted rain events. For the damage estimates contamination is not considered for rainfall inputs from radar, rainfall forecasts, FC1845 and FC1850. The damage is shown as mean damage per residential building in Euro.

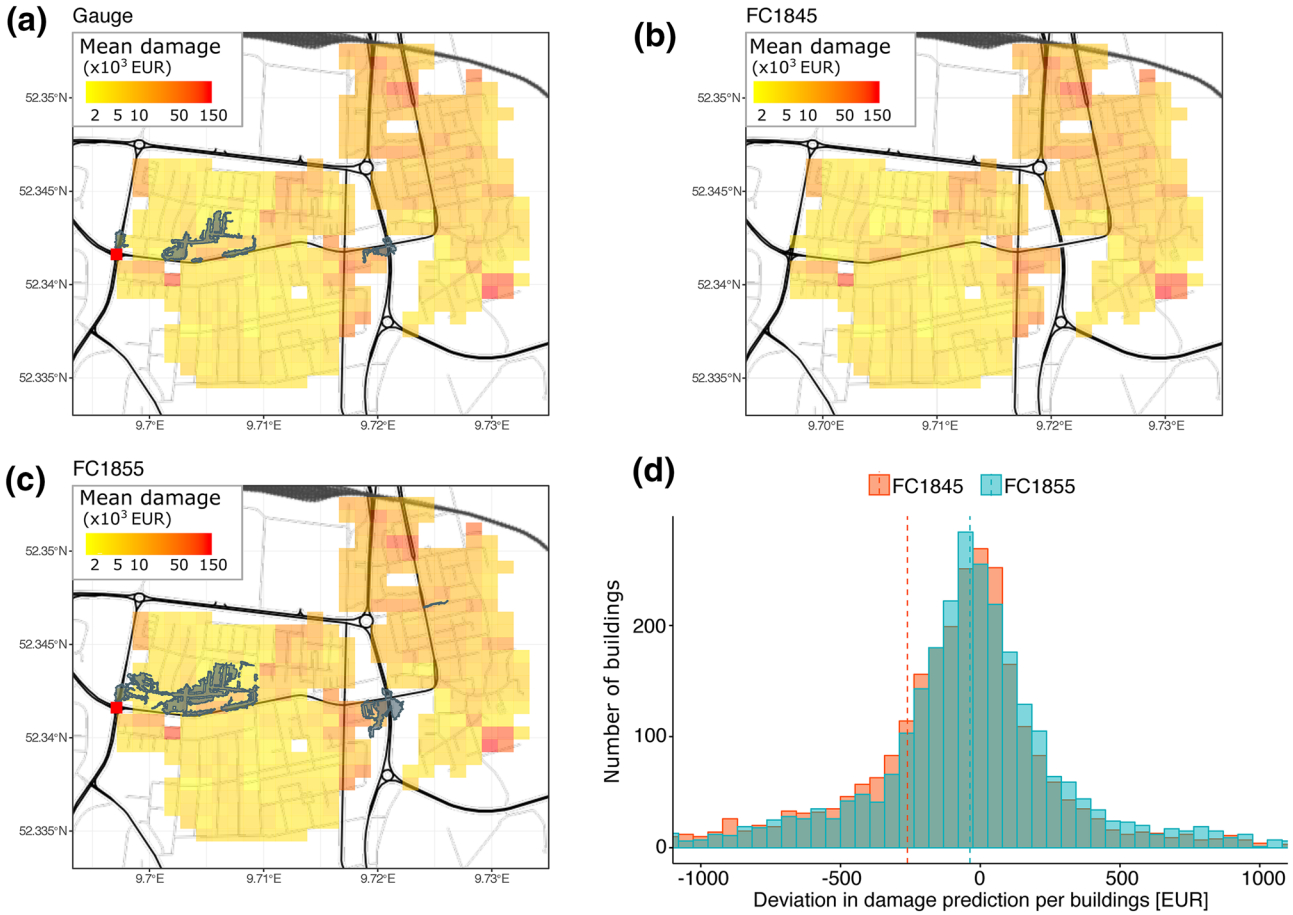

Figure 7. (a–c) Spatial distribution of mean damage to residential buildings (shown in yellow-red gradient) using inundation input from ANN model based on rainfall gauge (A-Gauge), rainfall forecast at 18:45 UTC (B-FC1845) and rainfall forecast at 18:55 UTC (C-FC1855). The contaminated area is shown accordingly in gray. The point of contaminant injection is shown as a red square. As the theoretical spill event was timed with the peak of the rainfall before 18:55 UTC, a prediction of the contaminated area is only available for the 18:55 UTC rainfall forecast (FC1855). (d) Deviation of predicted building damage for each residential building in the test area between gauge input (Gauge) and forecasts at 18:45 UTC (FC1845-red) and 18:55 UTC (FC1855-blue). ANN, artificial neural network; FC, forecast times.

the damage is validated on the household level for the June 22 pluvial flood event in Hannover using self-reported information on inundation, contamination, household size and knowledge of the flood risk of 12 randomly selected residential buildings affected during the event based on a post event online survey of private households. For the validation exercise the damage model is run with the reported information of the randomly selected households and the modeled damage estimates are compared against the reported damage values of those households. The mean absolute error of the modeled damage estimates for the buildings from the survey is EUR 1230. The hit rate, meaning the percentage of buildings for which the 90% predictive interval covers the reported damage, is 83%. In addition to the household-level validation, we find that the estimated mean building damage values for all affected buildings in our test area, which are in the range of EUR 4539 to EUR 4677, agree well with the average claims value for natural hazard events between 2007 and 2016 in this area and are also in all cases covered by the 90% predictive intervals of the predictions (between EUR 3193 and EUR 4279 on average for the federal state of Lower Saxony [GDV, 2019]). This provides a good indication that the outputs of the damage prediction can be seen as reliable estimates for the expected damage to residential buildings from pluvial floods.

The overall calculation time for the entire forecasting system as well the calculation times for each component using a standard desktop PC with four processing units is shown in Table 1. The calculation time for the entire forecasting system for the 5 km^2 test area in Hannover is less than 5 min, with the ANN inundation model taking around 20 s. This means that the ANN model needs only 0.13% of the calculation

time of the physically based hydraulic model. For the event in Hannover, this would allow to issue a first impact-based warning including a forecast of the inundated and contaminated areas as well as the expected losses to residential buildings just before the peak of the rainfall event at 18:55 UTC. It would further allow to issue an updated near-real time impact assessment every 5 min using just one standard desktop PC.

5. Discussion

The application and validation of the presented model chain shows that impact-based pluvial flood forecasting as part of an early warning system is feasible despite the complex hydrologic and hydraulic characteristics as well as the high spatial variability in exposure and vulnerability in urban areas. By replacing the commonly used coupled 2D hydraulic surface-subsurface models for modeling the flood inundation in urban areas with a novel data driven model based on artificial-neural-networks (ANN), we are able to significantly reduce the run-time of the model chain and hence remove the biggest bottleneck in providing timely inundation forecasts for impact based early warning systems. With less than 5 min computation time of the entire model chain on a standard desktop PC for a 5 km^2 urban catchment, warnings based on the provided impact forecasts could still be issued with a few minutes lead time to guide ad-hoc risk reduction measures and damage containment, which has not been possible with previous approaches. Apart from its use as part of an early warning system, the provided model outputs can provide important information for the immediate emergency response, which can help to improve capacity planning for emergency responders and support search and rescue operations (Estrany et al., 2020). Comparing the results of the ANN model with a physically based coupled 2D hydraulic surface-subsurface model for an actual pluvial event, we show that the deviations are only minor and hardly affect the performance of the subsequent models, namely the contaminant transport and damage model.

However, the performance of the inundation and subsequent damage and contaminant transport models require rainfall forecasts that accurately predict both the expected volume as well as its spatio-temporal distribution. The accuracy of these rainfall forecasts still vary considerably leading to often very short lead times, especially for convective rainstorms which are often responsible for pluvial flooding. For instance the hindcast of the rainstorm used in this study showed that rainfall forecasts were not reliable enough to be used for the impact based forecasting system until 5 min before the start of the rainfall event, which would allow to issue a first warning just at the start of the rain event. While this could still give emergency responders enough time to better prepare for incoming emergency calls or to improve action planning as well as for residents to seek shelter in a safe place, it might be too short to effectively prevent damage. Hence, improved forecasts of the spatio-temporal distribution of high intensity rainstorms would significantly boost the the effective use of impact-based forecasting systems to reduce damage.

While the presented ANN model was able to accurately predict the depth and extent of the inundation at a fraction of the time needed by a physically based model, the predictive skill of such data driven models using modern machine learning approaches, highly depends on the available data the model can be trained with. In this study a very detailed coupled 2D surface, 1D sewer network flow and full subsurface flow model was set up in the test area and run over several weeks using a large number of rainfall scenarios to generate a high quality training data set. While a model transfer to another urban area would require the training of a new ANN model or at least an update of the spatial dependency using local training data, it could still be part of a more cost-efficient and effective early warning solution than complex sensor networks frequently used in flash flood early warning systems (Acosta-Coll et al., 2018). An update instead of training a new ANN would be possible under the assumption that the ANN trained for the test area in this study would be able to reproduce the general behavior of pluvial floods in other urban areas. This is especially true in cases where inundation models already exist for the calculation of pluvial flood hazard and risk maps and therefore only need to be re-run with different rainfall scenarios to create a sufficiently large training data set for the ANN model.

Although the maps of contaminated areas produced by the contaminant transport model showed a good overlap between the forecasted contaminated area and the contaminated area based on flow fields from the hydraulic model, despite a relatively strong tendency to overestimate the contaminated area, its actual accuracy for a real contamination event could not be validated due to missing information on any contamination

that might have happened during the event. While a detailed validation of the predictions for contaminated areas is challenging, as it would require tracer experiments during a pluvial flood event in an urban area, the performed sensitivity analysis gives an indication about the magnitude with which contaminants are spreading during pluvial flood events. Such information is of great importance for both early warning and emergency response as contamination with for example sewage was found to be both a major health risk and important driver of damages to built assets during pluvial flood events. In case the presented forecast model is extended to an operational early-warning system, this information would need to be reported by eye-witnesses or emergency responders to be included in the impact forecast as information about spills or other contamination events is otherwise difficult to obtain. The cross platform mobile application developed alongside this impact based forecasting system is able to collect such information through volunteered geographic information but was not yet operational by the time of the event (see Appendix for detailed information on the proposed application and technical set up). While empirical evidence on how quickly such information could be collected in case of an emergency is currently lacking, the concept of an interactive two-way system that is able to send warnings to mobile devices and at the same time allows recipients to report or validate information, has big potential to provide more effective and meaningful warnings for pluvial floods. Such a system would at the same time allow to collect data comparable to those shown in Figure 4, which can be used to further calibrate and improve the accuracy of the outputs of such an early warning system.

While the mean damage predictions for residential buildings are in good agreement with the model benchmark, the reported damage from households for the modeled event as well as the long term average claims data, even for the early inundation forecasts, the variability and uncertainty of damage estimates on the property scale can be high (see Figure 7d). A large part of this uncertainty and variability is driven by predictions of the maximum water level as the most important predictor due to a number of assumptions that have to be made such as the relationship between the water outside and inside the building as well as the presence of a basement, but also a lack of detailed information on exposure and value of a building play a role. By using a probabilistic damage model in our early warning system, we can to some extent express these uncertainties in the damage estimates, which helps to translate inundation, exposure and vulnerability information into a meaningful spatial distribution of expected damage, despite the mentioned caveats. This information is particularly helpful to prioritize efforts in reducing and containing damage given that residents in urban areas commonly overestimate the probability of flooding, but frequently underestimate the potential damage (Botzen et al., 2015). Forecasted impact maps, including, for example information about monetary damage to buildings or damage hotspots, could substantially improve emergency response in respect to location, time and type of emergency measures (Bachmann et al., 2016; Bhola et al., 2018; Coles et al., 2017). Flood event managers, who need to assess, in real time, the severity of possible field consequences associated with floods, to be able to take appropriate decisions, would be better informed (Dale et al., 2014). Prototype systems have already been implemented in several test areas, for example in France, the Netherlands or Italy (Bachmann et al., 2016; Le Bihan et al., 2017). Although uncertainty of predictions is addressed in the damage model, it is not part in any of the other model parts. It would go beyond this proof-of-concept study to analyze the uncertainties of pluvial flood predictions and address the question of how to include them into impact-based forecasts and subsequently in an early warning system, however, it should be noted that the question is very relevant and further research in this direction would be useful. While pluvial floods can cause both direct and indirect damage, such as business or traffic interruptions, damage estimates in this study are limited to direct damage to residential buildings. While this covers the majority of damage in the residential test area in this study, other types of damage could in theory be included in the forecasting system. This however would require different types of damage models that could also account for indirect and consequential damage, which is beyond the scope of this proof-of-concept study.

Although a crowd sourcing model and cross-platform mobile early warning app (see Appendix for details) were readily developed, the system was not yet operational and fully coupled with the presented forecasting system by the time of the event. In order to be able to report on the effectiveness of the entire impact-based early warning system as outlined in Figure 1, including false-alarm rates, average lead times and response of different user groups, long term studies of the operational system would be necessary, which is beyond the scope of this study. The proposed approach would allow to integrate information from volunteers including relevant social media posts which could be utilized to deliver timely ground-truth information for

the impact based forecasts. Such an opportunistic data gathering relies on the willingness of volunteers to provide the location of their post—which is currently not very common among users in Germany. If the location of the post is available, the approach presented in detail in Feng and Sester (2018) is able to identify relevant posts reliably. As described above, this information could be used to verify the results of the models. However, a completely automated implementation of such an approach would require an automatic retrieval of e.g. water depth information from text or images, which is still in its early stages (Griesbaum et al., 2017), as well as a better understanding about the quality of the provided direct VGI data.

6. Conclusion

This study demonstrates that impact based forecasts for pluvial floods for use in an early warning system are feasible despite the high requirements for spatio-temporal resolutions of the input data and the typically short lead times. We test the developed impact-based forecasting system by hindcasting the rainfall field, inundated areas and water levels as well as the spreading of contaminants and direct damage to residential buildings for a real pluvial flood event that caused significant disruption in an urban area in Germany. A comparison of the outputs of the forecasting system with observed and modeled validation records showed a good agreement for forecasts made 5 min before the peak of the rain event. The data-driven inundation model based on an ANN can plausibly reproduce the flood inundation of a coupled physically based 2D hydraulic surface-subsurface model requiring a fraction of both the computational expense and time and by that removing one of the key obstacles in providing timely impact-based warnings in highly complex urban catchments. Deviations between the outputs of the model chain and the validation data can be mainly attributed to the high uncertainties in the rainfall forecasts. Therefore, we conclude that improving both the lead time and accuracy of rainfall forecasts could significantly boost the performance of impact-based pluvial flood forecasting systems needed for an efficient early warning. However, more detailed validation data on inundation, spreading of contaminants and resulting damage is needed to fully verify the reliability and sensitivity of each model component. In order to collect these data, we present and discuss the concept of a two-way early warning system with which the created outputs in the form of inundation, contamination and damage maps can be disseminated while at the same time near-real time validation data through volunteered geographic information from eye-witnesses can be collected. While more research is needed on how the integration of such a concept in an operational early warning system can be best utilized for different user groups and contexts, the presented impact based early forecasting system and early warning concept is an important step to provide meaningful warnings for pluvial floods which is needed both by the general public and emergency responders to effectively reduce damage and protect lives.

Data Availability Statement

The majority of the datasets used in this study are publicly available and can be accessed through public repositories. All used data repositories are cited either in the main text or in the supporting information. Table S1 additionally provides a list of all data sets used in the paper, their license and access restrictions as well as a description on how to access the data. Following data sets can be accesses with some restrictions: The precipitation data from the Stadtentwässerung Hannover can be accessed by researchers and the general public from Stadtentwässerung Hannover for noncommercial purposes on request. The pipe network can be accessed from the Stadtentwässerung Hannover for noncommercial purposes but requires accreditation by the Stadtentwässerung Hannover as the data is confidential due to public safety reasons. The building footprint data can be accessed from the Federal Agency for Cartography and Geodesy (BKG) free of charge for federal agencies and research institutes in Germany. Researchers with other affiliations can request access to the data through the link provided in Table 1 of the supporting information and after paying a service charge.

Acknowledgments
The research presented in this study was mainly conducted under the framework of the project "EVUS—Real-Time Prediction of Pluvial Floods and Induced Water Contamination in Urban Areas" (BMBF, 03G0846B). The authors would like to acknowledge the Stadtentwässerung Hannover who supported our work by providing the pipe network model and precipitation data. Additional financial support for V.R. by the Z Zurich Foundation, the Grantham Foundation for the Protection of the Environment and the ESRC via the Centre for Climate Change Economics and Policy under Grant number: ES/R009708/1 is gratefully acknowledged. Open access funding enabled and organized by Projekt DEAL.

References

Acosta-Coll, M., Ballester-Merelo, F., Martinez-Peiró, M., & De la Hoz-Franco, E. (2018). Real-time early warning system design for pluvial flash floods—a review. *Sensors*, *18*(7), 2255. https://doi.org/10.3390/s18072255

Bachmann, D., Eilander, D., De Leeuw, A., De Bruijn, K., Diermanse, F., Weerts, A., & Beckers, J. (2016). Prototypes of risk-based flood forecasting systems in the Netherlands and Italy. E3s web of conferences (Vol. *7* pp. 18018).

Berkhahn, S., Fuchs, L., & Neuweiler, I. (2019). An ensemble neural network model for real-time prediction of urban floods. *Journal of Hydrology*, *575*, 743–754.
Bermúdez, M., Ntegeka, V., Wolfs, V., & Willems, P. (2018). Development and comparison of two fast surrogate models for urban pluvial flood simulations. *Water Resources Management*, *32*(8), 2801–2815.
Berndt, C., Rabiei, E., & Haberlandt, U. (2014). Geostatistical merging of rain gauge and radar data for high temporal resolutions and various station density scenarios. *Journal of Hydrology*, *508*, 88–101.
Bhola, P. K., Leandro, J., & Disse, M. (2018). Framework for offline flood inundation forecasts for two-dimensional hydrodynamic models. *Geosciences*, *8*(9), 346.
Blake, E., & Zelinsky, D. (2018). *Tropical cyclone report hurricane harvey*. (Tech. Rep. No. AL092017). Miami, FL: National Hurricane Center.
BMVI (2012). *Richtlinie zur ermittlung des sachwerts sachwertrichtlinie–sw-rl*. (Tech. Rep. No. SW 11–4124.4/2). Berlin: Bundesministerium für Verkehr, Bau und Stadtentwicklung.
Bolle, A., das Neves, L., Smets, S., Mollaert, J., & Buitrago, S. (2018). An impact-oriented early warning and Bayesian-based decision support system for flood risks in Zeebrugge harbour. *Coastal Engineering*, *134*, 191–202.
Botzen, W. W., Kunreuther, H., & Michel-Kerjan, E. (2015). Divergence between individual perceptions and objective indicators of tail risks: Evidence from floodplain residents in New York city. *Judgment and Decision Making*, *10*(4), 365–385.
Chang, F.-J., Chen, P.-A., Lu, Y.-R., Huang, E., & Chang, K.-Y. (2014). Real-time multi-step-ahead water level forecasting by recurrent neural networks for urban flood control. *Journal of Hydrology*, *517*, 836–846.
Coles, D., Yu, D., Wilby, R. L., Green, D., & Herring, Z. (2017). Beyond 'flood hotspots': Modelling emergency service accessibility during flooding in New York, UK. *Journal of Hydrology*, *546*, 419–436.
Coulthard, T., & Frostick, L. (2010). The hull floods of 2007: Implications for the governance and management of urban drainage systems. *Journal of Flood Risk Management*, *3*(3), 223–231.
Dale, M., Wicks, J., Mylne, K., Pappenberger, F., Laeger, S., & Taylor, S. (2014). Probabilistic flood forecasting and decision-making: An innovative risk-based approach. *Natural Hazards*, *70*(1), 159–172.
Deshons, P., & Delrieu, G. (2002). *Urban flood management in Marseille (France): The case study of 19 Septembre 1999: Advances in flood forecasting, flood warning and emergency management, Barcelona, Spain*.
Estrany, J., Ruiz-Pérez, M., Mutzner, R., Fortesa, J., Nácher-Rodríguez, B., Tomàs-Burguera, M., et al. (2020). Hydrogeomorphological analysis and modelling for a comprehensive understanding of flash-flood damage processes: The 9 October 2018 event in Northeastern Mallorca. *Natural Hazards and Earth System Sciences*, *20*(8), 2195–2220.
Feng, Y., Brenner, C., & Sester, M. (2018). Enhancing the resolution of urban digital terrain models using mobile mapping systems. *ISPRS Annals of Photogrammetry, Remote Sensing and Spatial Information Sciences*, *IV-4/W6*, 11–18.Retrieved from https://www.isprs-ann-photogramm-remote-sens-spatial-inf-sci.net/IV-4-W6/11/2018/doi:10.5194/isprs-annals-IV-4-W6-11-2018
Feng, Y., & Sester, M. (2018). Extraction of pluvial flood relevant volunteered geographic information (VGI) by deep learning from user generated texts and photos. *ISPRS International Journal of Geo-Information*, *7*(2), 39.
GDV (2019). *Naturgefahrenreport 2018–serviceteil (Tech. Rep.)*. Berlin: Gesamtverband der Deutschen Versicherungswirtschaft e. V.
Ghimire, B., Chen, A. S., Guidolin, M., Keedwell, E. C., Djordjević, S., & Savić, D. A. (2013). Formulation of a fast 2D urban pluvial flood model using a cellular automata approach. *Journal of Hydroinformatics*, *15*(3), 676–686.
Grahn, T., & Nyberg, L. (2017). Assessment of pluvial flood exposure and vulnerability of residential areas. *International Journal of Disaster Risk Reduction*, *21*, 367–375.
Griesbaum, L., Marx, S., & Höfle, B. (2017). Direct local building inundation depth determination in 3-D point clouds generated from user-generated flood images. *Natural Hazards and Earth System Sciences*, *17*(7), 1191–1201.
Grünewald, U., Schümberg, S., Wöllecke, B., Graf-van Riesenbeck, G., & Piroth, K. (2009). Gutachten zur entstehung und verlauf des extremen niederschlag-abfluss-ereignisses am 26.07.2008 im stadtgebiet von dortmund–einschließlich der untersuchung der funktionsfähigkeit von wasserwirtschaftlichen anlagen und einrichtungen der stadt. In *Emschergenossenschaft und Dritter in den Gebieten Dortmund-Marten,-Dorstfeld und-Schönau, Gutachten im Auftrag der Stadt Dortmund und der Emschergenossenschaft*.
Henonin, J., Russo, B., Mark, O., & Gourbesville, P. (2013). Real-time urban flood forecasting and modelling–a state of the art. *Journal of Hydroinformatics*, *15*(3), 717–736.
ITWH (2019). *HYSTEM-EXTRAN 2D Modellbeschreibung (HYSTEM-EXTRAN 2D model description) [Computer software manual]*. Hannover: Institut Für Technisch-Wissenschaftliche Hydrologie GmbH.
Judi, D. R., Burian, S. J., & McPherson, T. N. (2010). Two-dimensional fast-response flood modeling: Desktop parallel computing and domain tracking. *Journal of Computing in Civil Engineering*, *25*(3), 184–191.
Krämer, S., Fuchs, L., & Verworn, H.-R. (2007). Aspects of radar rainfall forecasts and their effectiveness for real time control-the example of the sewer system of the city of Vienna. *Water Practice and Technology*, *2*(2).wpt2007042
Lamb, R., Crossley, M., & Waller, S. (2009). A fast two-dimensional floodplain inundation model. *Proceedings of the institution of civil engineers-water management*, *162*, 363–370.
Laudan, J., Rözer, V., Sieg, T., Vogel, K., & Thieken, A. H. (2017). Damage assessment in braunsbach 2016: Data collection and analysis for an improved understanding of damaging processes during flash floods. *Natural Hazards and Earth System Sciences*, *17*, 2163–2179.
Le Bihan, G., Payrastre, O., Gaume, E., Moncoulon, D., & Pons, F. (2017). The challenge of forecasting impacts of flash floods: Test of a simplified hydraulic approach and validation based on insurance claim data. *Hydrology and Earth System Sciences*, *21*(11), 5911.
Leitão, J., Simões, N., Maksimović, Č., Ferreira, F., Prodanović, D., Matos, J., & Marques, A. S. (2010). Real-time forecasting urban drainage models: Full or simplified networks? *Water Science and Technology*, *62*(9), 2106–2114.
Morsy, M. M., Goodall, J. L., O'Neil, G. L., Sadler, J. M., Voce, D., Hassan, G., & Huxley, C. (2018). A cloud-based flood warning system for forecasting impacts to transportation infrastructure systems. *Environmental Modelling & Software*, *107*, 231–244.
Neal, J., Fewtrell, T., & Trigg, M. (2009). Parallelisation of storage cell flood models using openMP. *Environmental Modelling & Software*, *24*(7), 872–877.
Ochoa-Rodríguez, S., Wang, L.-P., Thraves, L., Johnston, A., & Onof, C. (2018). Surface water flood warnings in England: Overview, assessment and recommendations based on survey responses and workshops. *Journal of Flood Risk Management*, *11*, S211–S221.
Ospina, R., & Ferrari, S. L. (2010). Inflated beta distributions. *Statistical Papers*, *51*(1), 111.
Papalexiou, S. M., & Montanari, A. (2019). Global and regional increase of precipitation extremes under global warming. *Water Resources Research*, *55*(6), 4901–4914. https://doi.org/10.1029/2018WR024067
Parker, D. J., Priest, S. J., & McCarthy, S. (2011). Surface water flood warnings requirements and potential in England and wales. *Applied Geography*, *31*(3), 891–900.

Peche, A., Graf, T., Fuchs, L., & Neuweiler, I. (2019). Physically based modeling of stormwater pipe leakage in an urban catchment. *Journal of Hydrology*, *537*, 778–793.

Rosenzweig, B. R., McPhillips, L., Chang, H., Cheng, C., Welty, C., Matsler, M., et al. (2018). Pluvial flood risk and opportunities for resilience. *Wiley Interdisciplinary Reviews: Water*, *5*(6), e1302.

Rözer, V., Kreibich, H., Schröter, K., Müller, M., Sairam, N., Doss-Gollin, J., et al. (2019). Probabilistic models significantly reduce uncertainty in hurricane harvey pluvial flood loss estimates. *Earth's Future*, *7*, 384–394. https://doi.org/10.1029/2018EF001074

Rözer, V., Müller, M., Bubeck, P., Kienzler, S., Thieken, A., Pech, I., et al. (2016). Coping with pluvial floods by private households. *Water*, *8*(7), 304.

Sämann, R., Graf, T., & Neuweiler, I. (2019). Modeling of contaminant transport during an urban pluvial flood event–the importance of surface flow. *Journal of Hydrology*, *568*, 301–310.

Shehu, B., & Haberlandt, U. (2017). Radar data quality impact on rainfall nowcasting for urban drainage application. In *International workshop on precipitation in urban areas*. Switzerland: Pontresina.

Spekkers, M., Kok, M., Clemens, F., & Ten Veldhuis, J. (2013). A statistical analysis of insurance damage claims related to rainfall extremes. *Hydrology and Earth System Sciences*, *17*(3), 913–922.

Tayfur, G., Moramarco, T., & Singh, V. P. (2007). Predicting and forecasting flow discharge at sites receiving significant lateral inflow. *Hydrological Processes: An International Journal*, *21*(14), 1848–1859.

Thieken, A. H., Müller, M., Kreibich, H., & Merz, B. (2005). Flood damage and influencing factors: New insights from the august 2002 flood in Germany. *Water Resources Research*, *41*(12), W12430. https://doi.org/10.1029/2005WR004177

Van Ootegem, L., Verhofstadt, E., Van Herck, K., & Creten, T. (2015). Multivariate pluvial flood damage models. *Environmental Impact Assessment Review*, *54*, 91–100.

Wang, K., Wang, L., Wei, Y.-M., & Ye, M. (2013). Beijing storm of July 21, 2012: Observations and reflections. *Natural Hazards*, *67*(2), 969–974.

Westra, S., Fowler, H., Evans, J., Alexander, L., Berg, P., Johnson, F., et al. (2014). Future changes to the intensity and frequency of short-duration extreme rainfall. *Reviews of Geophysics*, *52*(3), 522–555.

Wojcik, O., Holt, J., Kjerulf, A., Müller, L., Ethelberg, S., & Mølbak, K. (2013). Personal protective equipment, hygiene behaviours and occupational risk of illness after July 2011 flood in Copenhagen, Denmark. *Epidemiology & Infection*, *141*(8), 1756–1763.

Zhou, Q., Mikkelsen, P. S., Halsnæs, K., & Arnbjerg-Nielsen, K. (2012). Framework for economic pluvial flood risk assessment considering climate change effects and adaptation benefits. *Journal of Hydrology*, *414*, 539–549.